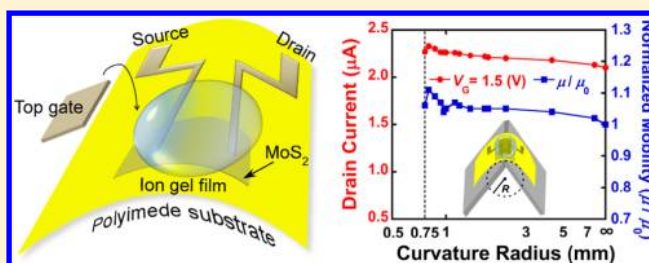


Highly Flexible MoS<sub>2</sub> Thin-Film Transistors with Ion Gel DielectricsJiang Pu,<sup>†</sup> Yohei Yomogida,<sup>†,‡</sup> Keng-Ku Liu,<sup>§</sup> Lain-Jong Li,<sup>\*,§</sup> Yoshihiro Iwasa,<sup>||,⊥</sup> and Taishi Takenobu<sup>\*,†</sup><sup>†</sup>Department of Applied Physics, Waseda University, Tokyo 169-8555, Japan<sup>‡</sup>Department of Physics, Graduate School of Science, Tohoku University, Sendai 980-8578, Japan<sup>§</sup>Institute of Atomic and Molecular Sciences, Academia Sinica, Taipei, 11529, Taiwan<sup>||</sup>Correlated Electron Research Group, RIKEN, Wako 351-0198, Japan<sup>⊥</sup>Quantum-Phase Electronics Center and Department of Applied Physics, The University of Tokyo, Tokyo 113-8656, Japan

## S Supporting Information

**ABSTRACT:** Molybdenum disulfide (MoS<sub>2</sub>) thin-film transistors were fabricated with ion gel gate dielectrics. These thin-film transistors exhibited excellent band transport with a low threshold voltage (<1 V), high mobility (12.5 cm<sup>2</sup>/(V·s)) and a high on/off current ratio (10<sup>5</sup>). Furthermore, the MoS<sub>2</sub> transistors exhibited remarkably high mechanical flexibility, and no degradation in the electrical characteristics was observed when they were significantly bent to a curvature radius of 0.75 mm. The superior electrical performance and excellent pliability of MoS<sub>2</sub> films make them suitable for use in large-area flexible electronics.

**KEYWORDS:** Two-dimensional material, transition metal dichalcogenide, molybdenum disulfide, electric double-layer transistor, flexible electronics



Two-dimensional (2D) atomically thin films are promising candidates for both nanoscale and flexible electronics applications, such as low-power, high-frequency, and flexible devices.<sup>1–6</sup> Graphene is the most widely explored 2D material because of its extremely high carrier mobility and unique physical properties, and the synthesis of large regions of graphene using chemical vapor deposition (CVD) is also currently feasible.<sup>4</sup> For example, graphene field-effect transistors fabricated on a plastic substrate have shown good mechanical flexibility and high carrier mobility. Most importantly, the performance of plastic-mounted graphene transistors exceeds that of other flexible materials, such as organic transistors (typically less than 1 cm<sup>2</sup>/(V·s)).<sup>4–8</sup> This novel development allowed innovations in the use of 2D materials for flexible applications; however, graphene is a zero-bandgap semiconductor. As a result, a graphene transistor typically exhibits a very low on/off current ratio, which limits the use of these materials for applications in logic electronics.

Recently, the transition metal dichalcogenide molybdenum disulfide (MoS<sub>2</sub>) has attracted considerable interest because of its stiffness, large intrinsic bandgap, and optical properties.<sup>1–3,9–12</sup> Transistors based on mechanically exfoliated MoS<sub>2</sub> monolayers have already been reported to exhibit a high current on/off ratio of  $1 \times 10^8$  and an electron mobility of 200 cm<sup>2</sup>/(V·s).<sup>2,3</sup> Very recently, the CVD growth of MoS<sub>2</sub> thin films that could be transferred onto other arbitrary substrates was reported, thereby providing a path forward to develop large-area electronics built onto a flexible plastic substrate.<sup>13,14</sup> Although the in-plane mechanical stiffness of MoS<sub>2</sub> thin films

has been determined to be as good as that of steel,<sup>9</sup> their electrical performance under severe bending has not yet been reported. Evaluation of the electrical performance of MoS<sub>2</sub> transistors that are integrated onto flexible substrates is just beginning.

Using MoS<sub>2</sub> in flexible devices requires gate materials that can be processed at low temperatures, that can be formed on plastic substrates, and that demonstrate mechanical flexibility. Currently, ion gels (gelation of an ionic liquid) have attracted considerable attention because of their printability, high ionic conductivity, large specific capacitance, and possible applicability to MoS<sub>2</sub> films.<sup>5,6,15–23</sup> MoS<sub>2</sub> electric double-layer transistors (EDLTs) formed with an ionic liquid have been successfully demonstrated, and ambipolar transport was observed.<sup>24</sup> Despite this great success, ionic liquids have significant limitations for flexible use because of the instability of the liquid body. This critical problem associated with liquids has recently been solved by gelation. An ion gel is capable of combining both the flexibility of an organic polymer dielectric and the high performance of an ionic liquid.

In this paper, we report the first MoS<sub>2</sub> EDLT using ion gel films as gate dielectrics. The MoS<sub>2</sub> thin films were grown using the scalable CVD method and then transferred onto other substrates, following ref 13 (Supporting Information S1). On

Received: April 9, 2012

Revised: July 11, 2012

Published: July 16, 2012

SiO<sub>2</sub> substrates, the MoS<sub>2</sub> EDLTs exhibited a low threshold, a high electron mobility, and a high on/off ratio. From the temperature dependence of the on and off current, we investigated the transport properties of MoS<sub>2</sub> EDLTs and observed an insulator-to-metal transition caused by the large accumulating carrier density, which is indicative of high levels of crystallinity and band transport in our CVD-grown MoS<sub>2</sub> film. On polyimide substrates, the MoS<sub>2</sub> EDLT exhibited remarkable electrical stability upon mechanical bending, and it exhibited a mechanical flexibility that was superior to that of graphene, carbon nanotubes, and oxide semiconductor films.

Figure 1a presents a schematic depiction of the MoS<sub>2</sub> EDLT with an ion gel. Highly crystalline MoS<sub>2</sub> thin films were grown

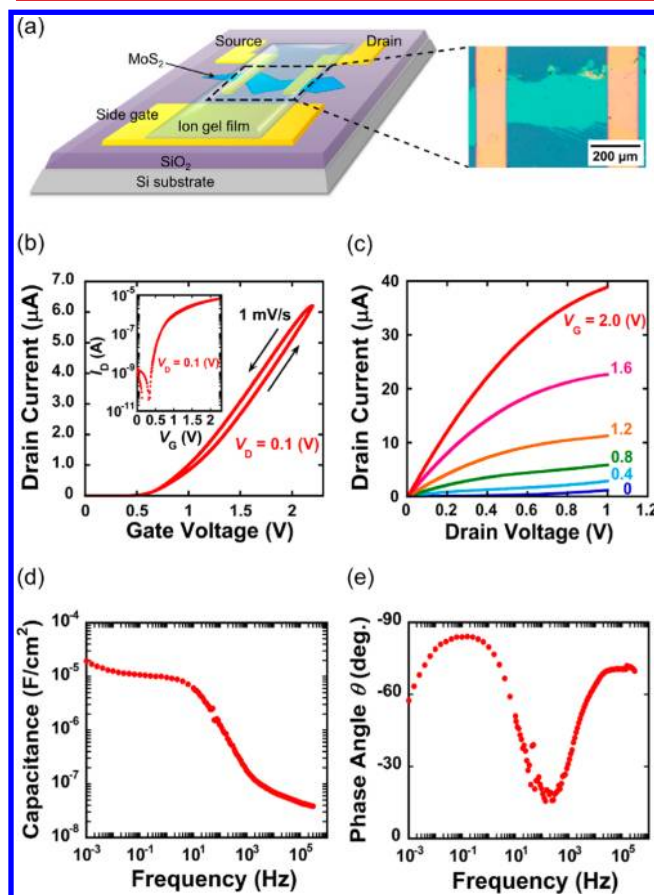


**Figure 1.** A thin-film MoS<sub>2</sub> EDLT constructed with an ion gel on a rigid substrate. (a) Schematic depiction and optical image of the MoS<sub>2</sub> EDLT. (b) Transfer and (c) output characteristics of the MoS<sub>2</sub> EDLT.  $V_D$  is the drain voltage, and  $V_G$  is the gate voltage. (d) Specific capacitance and (e) phase angle of the ion-gel/MoS<sub>2</sub> interface capacitor as a function of the applied frequency.

using a technique described by Liu et al.<sup>14</sup> We produced MoS<sub>2</sub> thin films on sapphire substrates through the high-temperature annealing of a thermally decomposed ammonium thiomolybdate layer in the presence of sulfur, and these films were transferred onto SiO<sub>2</sub>/Si substrates. The large-area CVD-grown MoS<sub>2</sub> films were identified to be trilayers based on AFM observation and Raman spectroscopy measurements (Supporting Information S2). Au films with Ni adhesion layers (50 nm/2 nm) were thermally deposited onto the top of the MoS<sub>2</sub> films as the source, drain, and side-gate electrodes. The ion gel films were fabricated from an ethyl propionate solution of the triblock copolymer poly(styrene-*block*-methylmethacrylate-

*block*-styrene) (PS-PMMA-PS,  $M_{PS}$  = 4.3 kg/mol,  $M_{PMMA}$  = 12.5 kg/mol,  $M_w$  = 21.1 kg/mol) and the ionic liquid 1-ethyl-3-methylimidazolium bis(trifluoromethylsulfonyl)imide ([EMIM][TFSI]).<sup>15–22</sup> The weight ratio of the polymer, ionic liquid, and solvent were maintained at 0.7:9.3:20. This solution was drop-cast onto the SiO<sub>2</sub>/Si substrate with the MoS<sub>2</sub> film and the electrodes. After evaporating the solvent, the electrical characterization was performed in a semiconductor parameter analyzer (Agilent E5270) using a shield probe station inside of a N<sub>2</sub>-filled glovebox. The transfer characteristics of a MoS<sub>2</sub> EDLT are presented in Figure 1b; the transistor performs as a typical n-type FET operating at a low gate voltage (0.68 V). The on/off current ratio reached 10<sup>5</sup> in these thin MoS<sub>2</sub> layers, which indicates a high switching property. As shown in Figure 1c, ideal ohmic-like contacts and a reasonable saturation behavior were observed, resulting in sufficient current amplification.

To correctly estimate the electron mobility, we measured the specific capacitance at the MoS<sub>2</sub>/ion-gel interface of our device, although the capacitance of the Au electrode/ion-gel interface with [EMIM][TFSI] has already been reported.<sup>17–22</sup> Impedance measurements were performed using a frequency response analyzer (a Solartron 1252A frequency response analyzer with a Solartron 1296 dielectric interface controlled by ZPlot and ZView software), and the frequency range was set to 10<sup>−3</sup>–10<sup>5</sup> Hz with an AC voltage amplitude of 10 mV; no DC voltage was applied. To obtain the capacitance of the MoS<sub>2</sub>/ion-gel surface, the source and drain electrodes were short-circuited, and two terminal measurements across the source/drain and side-gate electrodes were performed. Figure 1d displays the frequency profile of the specific capacitance. The capacitance at 0.1 Hz is 10.7 μF/cm<sup>2</sup>, and this is reasonably close to that of a metal surface (typically 5–10 μF/cm<sup>2</sup>).<sup>17–22</sup> Figure 1e shows the phase angle as a function of the applied frequency, and these results strongly suggest that the obtained capacitance measurements at 0.1 Hz are reasonable because a phase angle of −90° corresponds to a purely capacitive response. As shown in Figure 1e, the phase signal begins to decrease at low frequencies (<0.1 Hz), and this decrease might be attributable to the voltage-induced tunneling current, the leakage current passing through the EDL interface and/or the pseudocapacitance resulting from chemical processes at the EDL interface.<sup>23</sup> From a simple calculation (capacitance × applied gate voltage), the estimated maximum sheet carrier density is  $1.34 \times 10^{14}$  charges/cm<sup>2</sup>. Using these results, we derived the mobility of our MoS<sub>2</sub> EDLT, 12.5 cm<sup>2</sup>/(V·s), from the slope of the transfer characteristics between the gate voltage of 1.5 and 2.0 V using the standard equation for the linear region,  $I_D = (\mu W V_D C_i / L)(V_G - V_{th})$ , where  $I_D$  is the drain current,  $\mu$  is the field-effect mobility,  $W$  is the channel width,  $V_D$  is the drain voltage,  $C_i$  is the specific capacitance of the dielectric,  $L$  is the channel length,  $V_G$  is the gate voltage, and  $V_{th}$  is the threshold voltage.

The resulting mobility of 12.5 cm<sup>2</sup>/(V·s) is higher than the value reported for CVD-grown MoS<sub>2</sub> film transistors gated by solid dielectrics (up to 6 cm<sup>2</sup>/(V·s)).<sup>14</sup> Because the quality of films is one of the most important parameters in carrier mobilities, these results indicate the higher film quality in the measured MoS<sub>2</sub> film. The other possibility is lower contact resistances in EDLTs due to extremely high carrier density. Moreover, the mobility of the MoS<sub>2</sub> EDLTs obtained by the CVD method is still lower than the mobility of the MoS<sub>2</sub> exfoliated from MoS<sub>2</sub> crystals (200 cm<sup>2</sup>/(V·s)).<sup>3</sup> In these

devices, they used single-layer MoS<sub>2</sub> and top-gate geometry with HfO<sub>2</sub> top dielectric. Although the CVD-grown MoS<sub>2</sub> exhibits smaller MoS<sub>2</sub> domain (grain) sizes in the film than that of single-layer MoS<sub>2</sub> (Supporting Information S3), it is very difficult to clarify the reason of mobility differences and the direct comparison between the top-gate EDLTs and top-gate HfO<sub>2</sub> transistors is an important future issue. In addition to the film quality and the device structure, in Figure 1a, the MoS<sub>2</sub> film is naturally patterned during the transfer process. These dirty edges and irregular shapes might affect the electrical characteristics, which is another possible reason for the mobility difference.

The relatively high mobility in CVD-grown polycrystalline films generates a considerable amount of interest in the carrier transport properties. To gain additional insight into these MoS<sub>2</sub> thin films, as shown in Figure 2a, we investigated the

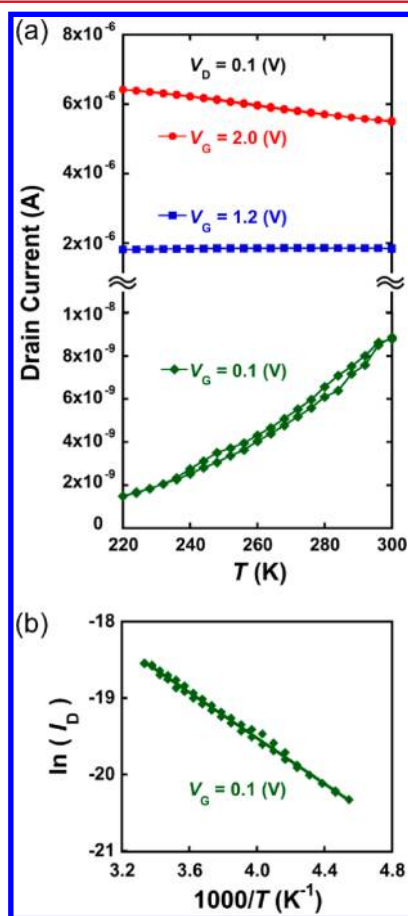


**Figure 2.** Metal-to-insulator transition observed in a thin-film MoS<sub>2</sub> EDLT constructed with an ion gel on a rigid substrate. (a) Temperature dependence of the drain current at a gate voltage,  $V_G$ , of 2.0 (red), 1.2 (blue), and 0.1 (green).  $V_D$  is the drain voltage. (b) Arrhenius plot of the drain current at  $V_G = 0.1$  V.

temperature dependence of the on-state and off-state drain currents. In the off-state (gate voltage of 0.1 V), the current decreased with temperature, indicating that the typical thermally activated behavior, which is commonly observed in semiconductors and insulators, was applicable in MoS<sub>2</sub> thin films. From the Arrhenius plot shown in Figure 2b, we can conclude that the transport mechanism in the off state involves thermal activity because we estimated an activation energy of 0.13 eV for the electron carriers. Because this energy is smaller

than the band gap of MoS<sub>2</sub> ( $\sim 1.2$  eV), it may correspond to the depth of the donor levels.<sup>11,12</sup> In sharp contrast to the insulating transport in the off state, as presented in Figure 2a, metal-like behavior was observed in the on state (gate voltage of 2.0 V) because the current was inversely proportional to the temperature. In the present results, the metal–insulator transition (MIT) was clearly demonstrated between the gate voltages of 0.1 and 2.0 V, and this MIT has already been reported in single-crystal MoS<sub>2</sub> thin flakes obtained by microcleavage, which was designed for the production of graphene.<sup>24</sup> The similarity between the single-crystal flakes and our CVD-grown thin films strongly suggests that the two exhibit comparable film qualities. Additionally, the band transport in the scalable CVD film demonstrates the limited influence of the domain boundaries on the carrier transport, although the CVD sample contains polycrystalline structures with grain sizes of approximately 10 nm (Supporting Information S3). Importantly, it is extremely difficult to obtain band transport in a typical flexible semiconducting film, such as those produced from organic materials.<sup>25</sup> These excellent transport properties in large-area films should prove to be a significant advantage for MoS<sub>2</sub> films when used in large-area flexible electronics. The MoS<sub>2</sub> films were transferred onto plastic substrates for further examination.

Figure 3a shows a schematic depiction of the device structure. We fabricated a MoS<sub>2</sub> EDLT on a very thin polyimide substrate (thickness of 12.5  $\mu\text{m}$ ). First, following ref 13, we transferred CVD-grown MoS<sub>2</sub> films onto polyimide substrates (Supporting Information S1). It should be noted that

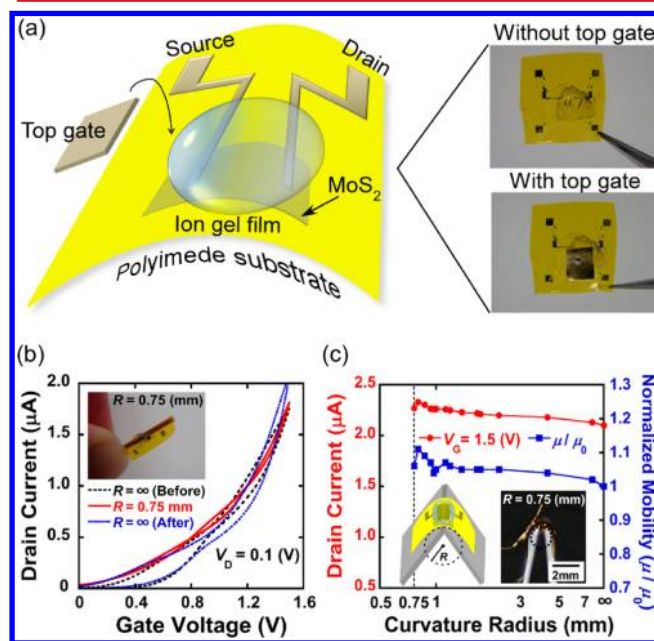


**Figure 3.** A thin-film MoS<sub>2</sub> EDLT constructed with an ion gel on a plastic substrate. (a) Schematic depiction and optical images of the MoS<sub>2</sub> EDLT. (b) Transfer characteristics of the MoS<sub>2</sub> EDLT. The red, black dotted, and blue dotted lines correspond to the transfer curve for a curvature radius of 0.75 mm and to the transfer curves before and after the bending experiments, respectively. The inset shows the optical image of the 0.75 mm curvature radius. (c) The dependence of the drain current at a gate voltage,  $V_G$ , of 1.5 V (red) and the carrier mobility on the curvature radius. The carrier mobility is normalized by the results without bending (blue). The inset schematically illustrates the bending measurements.



the transfer process from sapphire substrates onto other substrates might induce defects to MoS<sub>2</sub> films and lower carrier mobilities. Au films with Ni adhesion layers (50 nm/2 nm) were thermally deposited on top of the MoS<sub>2</sub> films as the source and drain electrode. Instead of a side-gate electrode, Au foil (thickness of 0.3 mm) was used as a top-gate electrode. The ion gel film solution was drop-cast onto the polyimide substrate with the MoS<sub>2</sub> film and electrodes. The capacitance of the ion-gel films on the polyimide substrates is 4.67  $\mu\text{F}/\text{cm}^2$  (at 1.0 Hz), and this value is also similar to that of a metal surface (typically 5–10  $\mu\text{F}/\text{cm}^2$ ).<sup>17–22</sup> Using these results, we derived the mobility of our MoS<sub>2</sub> EDLT on flexible substrates as 3.01  $\text{cm}^2/(\text{V}\cdot\text{s})$  from the slope of the transfer characteristics between 1.1 and 1.5 V. The on/off current ratio reached 10<sup>3</sup>. Note that because our MoS<sub>2</sub> film on the polyimide substrate is not patterned, we used the size of the electrode on the MoS<sub>2</sub> film as the channel width ( $W = 1150\ \mu\text{m}$ ) and the distance between the two electrodes as the channel length ( $L = 480\ \mu\text{m}$ ). For more accurate mobility calculations, we would need to pattern the MoS<sub>2</sub> film to isolate the channel region. One of the possible reasons for the obvious mobility difference between the MoS<sub>2</sub> film on the SiO<sub>2</sub> and that on the polyimide substrate might be the effect of the substrates.

To evaluate the mechanical flexibility of this device, the polyimide substrate was bent so that it was perpendicular to the direction of the drain current. The in situ bending test was performed in a glovebox using a home-built bending apparatus. Figure 3b shows the transfer curves of three bending conditions. Importantly, we did not observe an obvious electrical degradation during our maximum bending condition (curvature radius of 0.75 mm). Figure 3c displays the curvature radius dependence of the on current and the carrier mobility, which is normalized by the value without bending. The variation of the on current and normalized mobility as a function of the device bending was within 10%, and the MoS<sub>2</sub> thin-film EDLTs show extremely high flexibility. Note that such a high-mechanical flexibility (sustainable at a curvature radius of less than 1 mm) has only been reported for organic materials with a well-designed, improved device structure.<sup>26</sup> To the best of our knowledge, this report highlights the most flexible transistor among inorganic materials, including graphene, carbon nanotubes, and oxide semiconductors.<sup>4–6,27–30</sup> Note that we have not observed clear degradation in the MoS<sub>2</sub> thin-film EDLTs, even at a curvature radius of 0.75 mm, which is the maximum bending limit for our apparatus. We anticipate that a much higher mechanical stability can be expected.

Finally, we will discuss the origin of the ultrahigh flexibility of the CVD-grown MoS<sub>2</sub> films. Some reasons for the extremely high flexibility of this material are the stiff chemical bonds in the Mo–S networks and their atomic-scale thickness. Thin and strong films have advantageous flexible properties. Another reason for the ultrahigh flexibility is the strong interaction among the MoS<sub>2</sub> domains, which is demonstrated in the observed band conduction from the transport measurements (Figure 2a). The second and third MoS<sub>2</sub> layers might assist carrier transport across the domain boundaries and relax permanent deformation by bending. Furthermore, the flexible nature of ion gel films is also an advantage for flexible devices. The formation of electric double layers is automatically achieved by applying an electric field to any semiconducting surface. Therefore, ion gels are some of the best dielectric materials for use in flexible and stretchable electronics.

In summary, we have fabricated CVD-grown MoS<sub>2</sub> thin-film EDLTs using an ion gel. We obtained excellent transistor performance, which is characterized by a high on/off ratio of approximately 10<sup>5</sup> and a mobility of approximately 12.5  $\text{cm}^2/(\text{V}\cdot\text{s})$  at a low operating voltage of 0.68 V. In addition, superior transport properties, supported by a metal–insulator transition, were observed, demonstrating yet another advantage over other flexible materials, such as organic films. We also evaluated the performance of MoS<sub>2</sub> EDLTs on polyimide substrates, and these devices exhibit excellent mechanical flexibility; the minimum bending radius is as small as 0.75 mm. The results of this study clearly demonstrate the numerous possibilities for large-area, high-performance flexible electronics constructed with MoS<sub>2</sub> thin films.

## ■ ASSOCIATED CONTENT

### Supporting Information

The method for transfer of CVD-grown MoS<sub>2</sub> onto other substrates, the AFM image and Raman spectrum of the MoS<sub>2</sub> film, and the grain size of the MoS<sub>2</sub> film from TEM observation. This material is available free of charge via the Internet at <http://pubs.acs.org>.

## ■ AUTHOR INFORMATION

### Notes

The authors declare no competing financial interest.

## ■ ACKNOWLEDGMENTS

T.T. was partially supported by a Grant-in-Aid (17069003 and 22656003) from MEXT, Japan, a Waseda University Grant (2011A-501), and the Funding Program for the Next Generation of World-Leading Researchers. Y.I. was supported by a Grant-in-Aid for Scientific Research (S) (21224009), by the FIRST Program from JSPS, and by SICORP from JST. L.J.L. acknowledges the support from the Academia Sinica and National Science Council in Taiwan (NSC-99-2112-M-001-021-MY3).

## ■ REFERENCES

- (1) Novoselov, K. S.; Jiang, D.; Schedin, F.; Booth, T. J.; Khotkevich, V. V.; Morozov, S. V.; Geim, A. K. *Proc. Natl. Acad. Sci. U.S.A.* **2005**, *102*, 10451–10453.
- (2) Schwierz, F. *Nat. Nanotechnol.* **2010**, *5*, 487–496.
- (3) Radisavljevic, B.; Radenovic, A.; Brivio, J.; Giacometti, V.; Kis, A. *Nat. Nanotechnol.* **2011**, *6*, 147–150.
- (4) Kim, K. S.; Zhao, Y.; Jang, H.; Lee, S. Y.; Kim, J. M.; Ahn, J. H.; Kim, P.; Choi, J. Y.; Hong, B. H. *Nature* **2009**, *457*, 706–710.
- (5) Kim, B. J.; Jang, H.; Lee, S. K.; Hong, B. H.; Ahn, J. H.; Cho, J. H. *Nano Lett.* **2010**, *10*, 3464–3466.
- (6) Lee, S. K.; Kim, B. J.; Jang, H.; Yoon, S. C.; Lee, C.; Hong, B. H.; Rogers, J. A.; Cho, J. H.; Ahn, J. H. *Nano Lett.* **2011**, *11*, 4642–4646.
- (7) Sun, J.; Zhang, B.; Katz, H. E. *Adv. Funct. Mater.* **2011**, *21*, 29–45.
- (8) Wen, Y. G.; Liu, Y. Q. *Adv. Mater.* **2010**, *22*, 1331–1345.
- (9) Bertolazzi, S.; Brivio, J.; Kis, A. *ACS Nano* **2011**, *5*, 9703–9709.
- (10) Castellanos-Gomez, A.; Poot, M.; Steele, G. A.; van der Zant, H. S. J.; Agrait, N.; Rubio-Bollinger, G. *Adv. Mater.* **2012**, *24*, 772.
- (11) Mak, K. F.; Lee, C.; Hone, J.; Shan, J.; Heinz, T. F. *Phys. Rev. Lett.* **2010**, *105*, 136805.
- (12) Eda, G.; Yamaguchi, H.; Voiry, D.; Fujita, T.; Chen, M. W.; Chhowalla, M. *Nano Lett.* **2011**, *11*, 5111–5116.
- (13) Lee, Y.-H.; Zhang, X. Q.; Zhang, W.; Chang, M.-T.; Lin, C.-T.; Chang, K.-D.; Yu, Y.-C.; Wang, J. T.-W.; Chang, C.-S.; Li, L.-J.; Li, T.-W. *Adv. Mater.* **2012**, DOI: DOI: adma201104798.

- (14) Liu, K. K.; Zhang, W.; Lee, Y. H.; Lin, Y. C.; Chang, M. T.; Su, C. Y.; Chang, C. S.; Li, H.; Shi, Y.; Zhang, H.; Lai, C. S.; Li, L. J. *Nano Lett.* **2012**, *12*, 1538–1544.
- (15) Susan, Md. A. B. H.; Kaneko, T.; Noda, A.; Watanabe, M. *J. Am. Chem. Soc.* **2005**, *127*, 4976.
- (16) Lee, J.; Panzer, M. J.; He, Y.; Lodge, T. P.; Frisbie, C. D. *J. Am. Chem. Soc.* **2007**, *129*, 4532.
- (17) Cho, J. H.; Lee, J.; Xia, Y.; Kim, B.; He, Y.; Renn, M. J.; Lodge, T. P.; Frisbie, C. D. *Nat. Mater.* **2008**, *7*, 900–6.
- (18) Cho, J. H.; Lee, J.; He, Y.; Kim, B. S.; Lodge, T. P.; Frisbie, C. D. *Adv. Mater.* **2008**, *20*, 686–690.
- (19) Xia, Y.; Zhang, W.; Ha, M.; Cho, J. H.; Renn, M. J.; Kim, C. H.; Frisbie, C. D. *Adv. Funct. Mater.* **2010**, *20*, 587–594.
- (20) Ha, M.; Xia, Y.; Green, A. A.; Zhang, W.; Renn, M. J.; Kim, C. H.; Hersam, M. C.; Frisbie, C. D. *ACS Nano* **2010**, *4*, 4388–4395.
- (21) Lee, J.; Kaake, L. G.; Cho, J. H.; Zhu, X.-Y.; Lodge, T. P.; Frisbie, C. D. *J. Phys. Chem. C* **2009**, *113*, 8972–8981.
- (22) Yomogida, Y.; Pu, J.; Shimotani, H.; Ono, S.; Hotta, S.; Iwasa, Y.; Takenobu, T. *Adv. Mater.* **2012**, DOI: DOI: adma.201200655.
- (23) Yuan, H.; Shimotani, H.; Ye, J.; Yoon, S.; Aliah, H.; Tsukazaki, A.; Kawasaki, M.; Iwasa, Y. *J. Am. Chem. Soc.* **2010**, *132*, 18402.
- (24) Zhang, Y.; Ye, J.; Matsushashi, Y.; Iwasa, Y. *Nano Lett.* **2012**, *12*, 1136–1140.
- (25) Braga, D.; Horowitz, G. *Adv. Mater.* **2009**, *21*, 1473–1486.
- (26) Sekitani, T.; Zschieschang, U.; Klauk, H.; Someya, T. *Nat. Mater.* **2010**, *9*, 1015–1022.
- (27) Park, J. U.; Nam, S.; Lee, M. S.; Lieber, C. M. *Nat. Mater.* **2012**, *11*, 120–125.
- (28) Takenobu, T.; Takahashi, T.; Kanbara, T.; Tsukagoshi, K.; Aoyagi, Y.; Iwasa, Y. *Appl. Phys. Lett.* **2006**, *88*, 033511.
- (29) Aikawa, S.; Einarsson, E.; Thurakitseree, T.; Chiashi, S.; Nishikawa, E.; Maruyama, S. *Appl. Phys. Lett.* **2012**, *100*, 063502.
- (30) Chien, C. W.; Wu, C. H.; Tsai, Y. T.; Kung, Y. C.; Lin, C. Y.; Hsu, P. C.; Hsieh, H. H.; Wu, C. C.; Yeh, Y. H.; Leu, C. M.; Lee, T. M. *IEEE Trans. Electron Devices* **2011**, *58*, 1440–1446.